Large Perturbations of the Carbon Cycle During Recovery from the End-Permian Extinction

Jonathan L. Payne,[1]* Daniel J. Lehrmann,[2] Jiayong Wei,[3] Michael J. Orchard,[4] Daniel P. Schrag,[1] Andrew H. Knoll[1]

High-resolution carbon isotope measurements of multiple stratigraphic sections in south China demonstrate that the pronounced carbon isotopic excursion at the Permian-Triassic boundary was not an isolated event but the first in a series of large fluctuations that continued throughout the Early Triassic before ending abruptly early in the Middle Triassic. The unusual behavior of the carbon cycle coincides with the delayed recovery from end-Permian extinction recorded by fossils, suggesting a direct relationship between Earth system function and biological rediversification in the aftermath of Earth's most devastating mass extinction.

The most severe extinction since the advent of animal life on Earth occurred at the end of the Permian Period, 251 million years ago (Ma) (1–3), with global loss of marine species estimated near 90% (4, 5). Organisms with heavy calcification and limited elaboration of circulatory and respiratory systems were most severely affected, whereas those with more active control of circulation, elaborated structures for gas exchange, and lightly calcified or uncalcified skeletons survived in much higher proportions (6). The ensuing Early Triassic was an interval of delayed biotic recovery characterized by continued low diversity (5); the persistence of a cosmopolitan fauna in the oceans (7); the absence of metazoan reefs (8), calcareous algae (9), calcareous sponges (10), and corals (11); the apparent absence of marine taxa recorded in both Permian and Middle Triassic rocks (12); a reduction in the size of invertebrates (13); and, on land, a hiatus in coal deposition (14). Sustained recovery of marine diversity and ecology began primarily in the early part of the Middle Triassic, some 4 to 8 million years after the extinction itself. The apparent delay of biological renewal could reflect the time scale necessary for reintegration of ecosystems (5, 12) or poor Early Triassic fossil preservation (12), but it has also been widely interpreted as a consequence of persistently unfavorable environmental conditions through part or all of the Early Triassic (5, 15, 16).
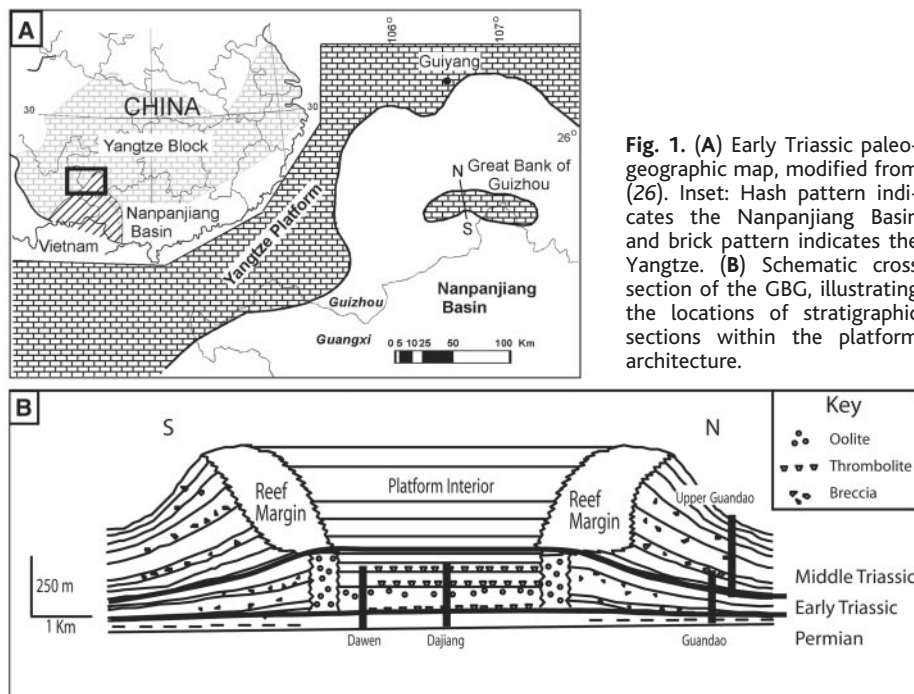
Aside from the extinction itself, the strongest evidence for environmental disturbance at the Permian-Triassic (P-Tr) boundary is a sharp negative excursion of 2 to 4 per mil (‰) in the carbon isotopic composition ($\delta^{13}C$) of marine carbonate ($\delta^{13}C_{carb}$) (17, 18) and one or more similar excursions in the $\delta^{13}C$ of organic matter ($\delta^{13}C_{org}$) (19–21). Although the apparent stabilization of $\delta^{13}C_{carb}$ above the boundary interval (17) has been used to suggest a stable but reduced fraction of organic carbon burial in the Early Triassic (22), the carbon isotopic record of Early and Middle Triassic rocks has received relatively little study. Positive carbon isotopic excursions have been noted at the Dienerian-Smithian (23), Smithian-Spathian (24), and Spathian-Anisian boundaries (25), but, to

date, the only complete Early and Middle Triassic carbon isotopic data set previously compiled from a single stratigraphic section is in an unpublished dissertation (23).

We sampled the Great Bank of Guizhou (GBG), an isolated Late Permian to Late Triassic carbonate platform in the Nanpanjiang Basin of Guizhou Province, southern China (Fig. 1A), to obtain high-resolution profiles of $\delta^{13}C_{carb}$ from the Late Permian through the Middle Triassic. The exposure of sections in both platform interior and basin margin settings further allows us to compare data across a range of depositional environments (Fig. 1B). A detailed stratigraphic framework for the platform has been developed from sequence stratigraphic (26), biostratigraphic, and geochronologic studies (27).

Our results show that the P-Tr boundary carbon isotope excursion was not an isolated event. Rather, it was the first in a series of (mostly larger) excursions that continued throughout the Early Triassic and into the early part of the Middle Triassic Period (Fig. 2). The excursions ended early in the Anisian (Bithynian) and were followed by an extended interval of stable values around 2‰. The interval of carbon-isotopic stability continued through the remainder of the Middle Triassic and into the Carnian (Fig. 3), demonstrating that the large fluctuations in $\delta^{13}C_{carb}$ are confined to Early Triassic strata.

Absolute ages of 251.4 ± 0.3 Ma (1) or ~253 Ma (2) for the P-Tr boundary and ~247 Ma for the Early-Middle Triassic boundary (27) constrain the entire Early Triassic to ~4.5 to 6 Ma and individual isotopic excursions to less than 1 million years in each

[1]Department of Earth and Planetary Sciences, Harvard University, 20 Oxford Street, Cambridge, MA 02138, USA. [2]Department of Geology, University of Wisconsin–Oshkosh, 800 Algoma Boulevard, Oshkosh, WI 54901, USA. [3]Guizhou Bureau of Geology and Mineral Resources, Bagongli, Guiyang 550011, Guizhou, People's Republic of China. [4]Geological Survey of Canada, 101-605 Robson Street, Vancouver, BC V6B 5J3, Canada.

*To whom correspondence should be addressed. E-mail: jpayne@fas.harvard.edu

Fig. 1. (A) Early Triassic paleogeographic map, modified from (26). Inset: Hash pattern indicates the Nanpanjiang Basin and brick pattern indicates the Yangtze. (B) Schematic cross section of the GBG, illustrating the locations of stratigraphic sections within the platform architecture.

case. The drops in $\delta^{13}C_{carb}$ at the P-Tr boundary and at the base of the overlying cyclic interval in the platform interior (Fig. 2) occur within 10 m of section, suggesting a very short time scale for these events, whereas the positive and negative excursions observed in the upper part of the platform interior and on the basin margin occur over longer stratigraphic intervals (>50 m), implying that they developed more slowly, although still in less than 1 million years. The symmetry of the positive and negative excursions indicates that the time scales of increases and decreases in $\delta^{13}C_{carb}$ were similar.

Our data (28) reproduce both the gradual carbon-isotopic drop in Late Permian oceans and the rapid negative excursion at the P-Tr boundary (17). The negative excursion at the base of the platform interior cyclic interval and the subsequent positive excursion are hinted at by basal Triassic $\delta^{13}C_{org}$ profiles for nonmarine successions (19), and they appear to correlate with data from the Italian Dolomites reported in an abstract (29). Our data also corroborate previous reports of positive excursions at the Smithian-Spathian (24) and Spathian-Anisian (25) boundaries, as well as the general shape of composite isotopic profiles developed from sections in Anhui Province, China (30), and multiple profiles reported from across the Tethys (23). The consistency of our findings with the more limited results from other areas, the sharp contrast between the Early and Middle Triassic

records on the GBG, and the consistency of the platform interior and basin margin records indicate that these data reflect global instability of the Early Triassic carbon cycle rather than local, diagenetic, or facies-specific effects. Confirmation of the global nature of the signal will depend upon additional high-resolution studies at other localities.

What physical mechanisms could have generated positive and negative isotopic shifts in $\delta^{13}C_{carb}$ of up to 8‰ in marine carbonates over time scales of tens to hundreds of thousands of years? Although the rapidity of the extinction (31) and isotopic excursion at the P-Tr boundary is compatible with emerging evidence of bolide impact (32, 33), the longer time scale of the subsequent excursions suggests another cause. Eruption of the Siberian Traps provides another possible explanation for prolonged instability in the carbon cycle. Available radiometric dates restrict Siberian trap basalts to the boundary interval itself (34), but the limited geographic scope of dated sections relative to the known area of the volcanic flows and the presence of >1000 m of flows above the youngest dated horizon (34) leave open the possibility that episodic eruption occurred through much of the Early Triassic. More age data are needed to test this scenario.

Massive methane release from sea-floor gas hydrate reservoirs has also been suggested as an explanation for the P-Tr boundary excursion (5, 19, 21, 35). Unlike the Late Paleocene event for which gas hydrate release was first proposed

(36), however, the more gradual and roughly symmetric increases and decreases in $\delta^{13}C_{carb}$ during the later part of the Early Triassic would require extended, alternating intervals of methane storage and release. The long time scale [>100 thousand years (ky), assuming constant sedimentation rates] of the negative shifts is difficult to account for under the scenario of methane release, because as the time scale of the isotopic shift increases, so too does the amount of methane needed to produce the same excursion. The ~8‰ drop from the late Dienerian to Smithian (Fig. 2) over 100 to 500 ky would require the release of much more than 10,000 Gt of methane (1 Gt = 10^7 kg) (37), more than five times the amount suggested to account for the Late Paleocene thermal maximum (36). Furthermore, the dependence of methane production on organic carbon burial precludes rapid (i.e., <1 million years) replenishment of the methane hydrate reservoir in the absence of extraordinarily high rates of organic carbon burial (38). Methane release is an attractive hypothesis for the P-Tr carbon-isotopic event viewed in isolation, but the full Early Triassic record is not easily reconciled with a methane-driven scenario.

Another explanation for the positive and negative excursions is that there were massive changes in the burial of organic carbon relative to carbonate carbon (f_{org}). Such an explanation requires periodic episodes of extraordinarily high organic carbon burial ($f_{org} > 0.5$, resulting in a positive shift in

Fig. 2. Carbon isotopic data from all sections and conodont ranges from Guandao section. The time scale is based on conodont and foraminiferal biostratigraphy from the Guandao section. Correlations from the basin margin to the platform interior are constrained by the occurrence patterns of Late Permian foraminifera (e.g., *Palaeofusulina* and *Colaniella*) and Griesbachian conodonts (*Hindeodus parvus* and *Isarcicella isarcica*) in the P-Tr boundary interval of the platform interior and by the occurrence of the Smithian conodont *Parachirognathus* (indicated by an asterisk) in the uppermost cyclic interval of Dawen and Dajiang sections. *Gd.*, *Gladiogondolella*; *Cs.*, *Chiosella*; *Ns.*, *Neospathodus*; *Ns. ex. gr.*, *Neospathodus ex grupo*; *Ng.*, *Neogondolella*; *Bith.*, Bithynian; *Aeg.*, Aegean.
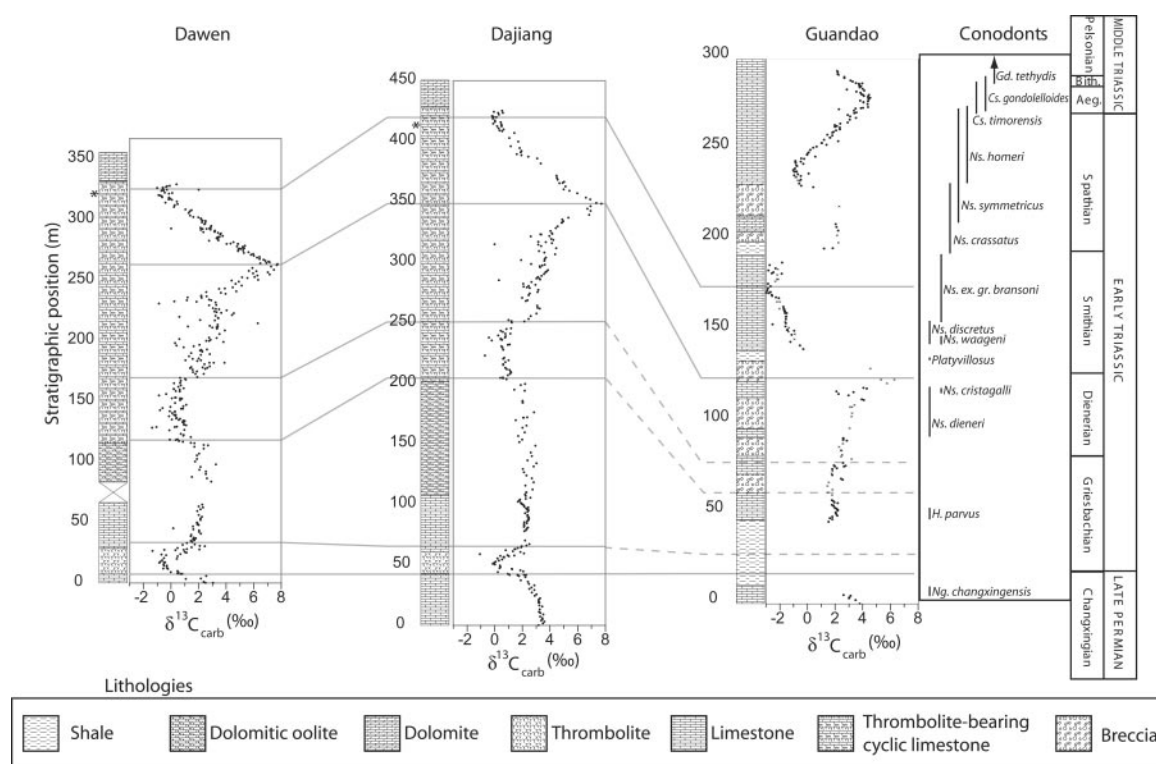
Fig. 3. Composite carbon isotopic curve for the Changxingian-Carnian (Cordevolian) compared to the pattern of biotic recovery from the end-Permian extinction. Lithostratigraphy and conodont ranges are shown for the Upper Guandao section. The conodont ranges are used to constrain the Middle and Late Triassic time scale. Radiometric dates are from (*1, 27, 44*), dasyclad algal diversity data from (*9*), coral and sponge diversity data from (*45*), and global diversity data from (*46*). Gastropod data are shown in table S1. Carbon isotope data: red, Guandao; blue, Dajiang; gold, Dawen; green, Upper Guandao. Fass., Fassanian; Long., Longobardian; *Ni.*, *Nicoraella*; *Pg.*, Paragondolella; *Bv.*, *Budurovignathus*; *M.*, *Metapolygnathus*; gen., number of genera; sp., number of species.
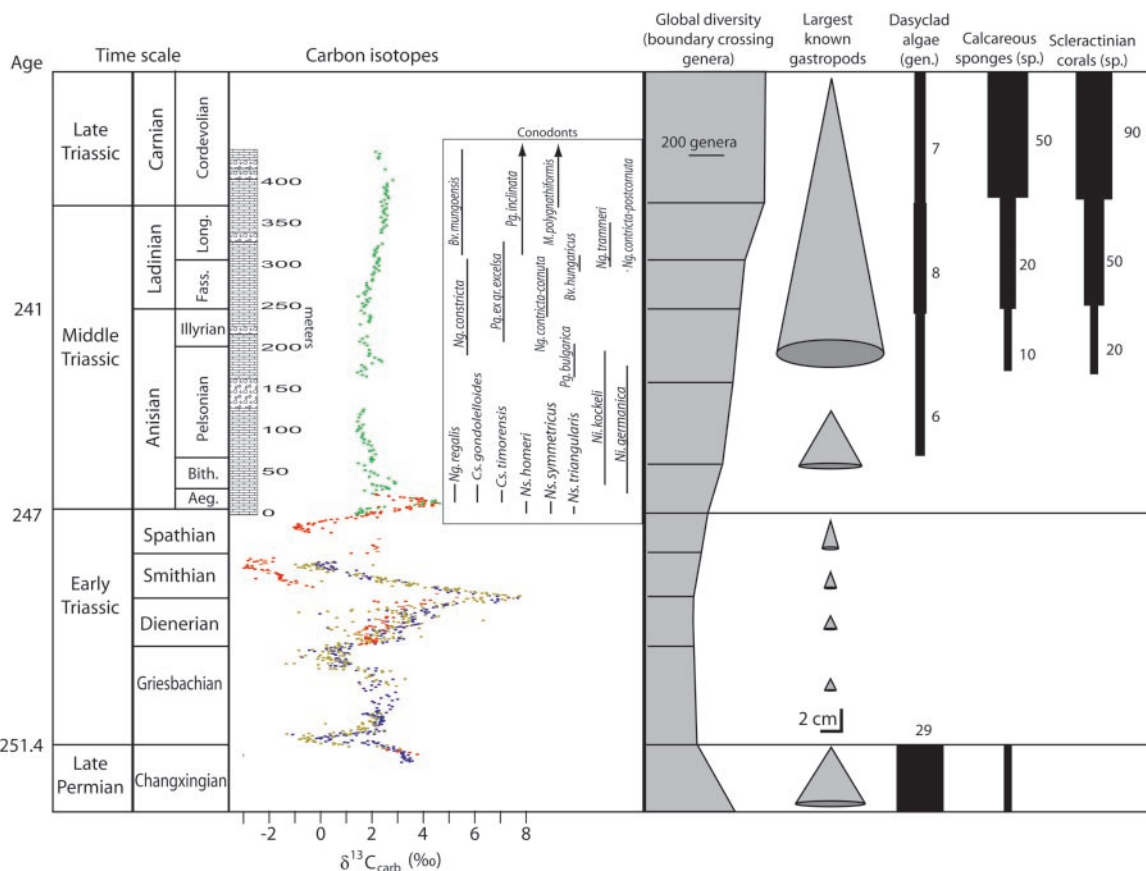
$\delta^{13}C_{carb}$) alternating with episodes of a much lower fraction of organic carbon burial ($f_{org} < 0.2$, resulting in a negative shift in $\delta^{13}C_{carb}$), a scenario that may also account for what has been observed in the carbon isotope record for the Neoproterozoic and Cambrian (*39, 40*). One hypothesis that has been proposed to explain very high $\delta^{13}C_{carb}$ values at those times was a more tropical continental configuration, such that tropical river deltas became anoxic, greatly increasing phosphate recycling and allowing very high rates of organic carbon burial (*37*). If correct, then perhaps the Early Triassic, tropical Tethys ocean basin alternated between oxic and anoxic conditions, with very large changes in organic burial rates. Alternatively, large variations in carbon burial fluxes may have resulted from mechanisms related to the low diversity of Early Triassic ecosystems. Regardless of the explanation, the close resemblance of the Early Triassic carbon isotope record with the repeated excursions recorded near the Neoproterozoic-Cambrian boundary (*39, 40*) may reflect similar forcing mechanisms.

The Early Triassic interval marked by repeated large and rapid isotopic excursions coincides with the paleontologically observed interval of limited biological recovery. Fossils provide several independent metrics of

recovery. After the decimation of Late Permian ecosystems, global diversity began to rise in the Smithian, with the largest and most rapid increase occurring in the early Anisian. Much anecdotal evidence indicates that body size in many invertebrate groups remained small throughout the Early Triassic (*13*). Figure 3, which includes a global compilation of maximum size in gastropods, provides quantitative confirmation of this phenomenon for one group. The reappearance of calcified green algae (*41*) also began in the Early Anisian (Aegean and Bithynian), coincident with carbon isotope stabilization. Scleractinian corals appeared, and heavily calcified sponges reappeared shortly thereafter, in the Pelsonian (*42*). The considerable Anisian diversity of dasyclad algae, scleractinian corals, and sponges reflects the nearly simultaneous resumption or acquisition of calcification in several lineages within these groups (*43*). Differences in physiological mechanisms of biomineralization may explain the slower time scale of skeletal (re)acquisition in previously uncalcified lineages of scleractinians and sponges versus algae.

The stratigraphic coincidence of large carbon isotope fluctuations with the protracted delay of biotic recovery from the end-Permian mass extinction suggests two classes of explanations. One possibility is that the carbon isotopic variations represent repeated

environmental disturbances that directly inhibited biotic recovery. If correct, then the disturbances must have followed one another with sufficient rapidity to preempt any visible recovery in the fossil record. This is consistent with the known paleontological pattern and can be tested by future refinements in the timing of first appearances of Middle Triassic scleractinian corals and sponges (i.e., they should post-date isotopic stabilization by an interval longer than the time between Early Triassic isotopic excursions). Another possibility is that the carbon isotope variations are, themselves, a consequence of decimated Early Triassic ecosystems, reflecting ecological controls on organic carbon burial. Whichever explanation is correct, the association between the most extreme carbon isotope excursions observed in the Phanerozoic Eon and the delayed recovery in the aftermath of Earth's largest mass extinction challenges our understanding of the ways that biological diversity and carbon cycling have interacted through Earth history.

References and Notes

1. S. A. Bowring *et al.*, *Science* **280**, 1039 (1998).
2. R. Mundil *et al.*, *Earth Planet. Sci. Lett.* **187**, 131 (2001).
3. References (*1*) and (*2*) report ages of 251.4 ± 0.3 Ma and ~253 Ma, respectively, for P-Tr boundary ash beds from the same locality. Because the only published age for the Early-Middle Triassic boundary was determined in the same laboratory as in (*1*), we have

chosen for consistency's sake to use the result from (*1*). The conclusions of this paper do not depend on which date is more accurate.

4. D. M. Raup, *Science* **206**, 217 (1979).
5. D. H. Erwin, *The Great Paleozoic Crisis: Life and Death in the Permian* (Critical Moments in Paleobiology and Earth History Series, Columbia Univ. Press, New York, 1993).
6. A. H. Knoll, R. K. Bambach, D. E. Canfield, J. P. Grotzinger, *Science* **273**, 452 (1996).
7. J. K. Schubert, D. J. Bottjer, *Palaeogeogr. Palaeoclimatol. Palaeoecol.* **116**, 1 (1995).
8. E. Flügel, in *Pangea: Paleoclimate, Tectonics, and Sedimentation During Accretion, Zenith, and Breakup of a Supercontinent*, G. D. Klein, Ed. (Geological Society of America, Boulder, CO, 1994), pp. 247–266.
9. E. Flügel, in *Paleoalgology: Contemporary Research and Applications*, D. F. Toomey, M. H. Nitecki, Eds. (Springer-Verlag, Berlin, 1985), pp. 344–351.
10. P. Riedel, B. Senowbari-Daryan, in *Fossil and Recent Sponges*, J. Reitner, H. Keupp, Eds. (Springer, Berlin, 1991), pp. 465–476.
11. G. D. Stanley, *Earth Sci. Rev.* **60**, 195 (2003).
12. D. H. Erwin, in *Evolutionary Paleobiology*, D. H. Erwin, D. Jablonski, J. H. Lipps, Eds. (Univ. of Chicago Press, Chicago, 1996), pp. 398–418.
13. R. J. Twitchett, *Palaeogeogr. Palaeoclimatol. Palaeoecol.* **154**, 27 (1999).
14. G. J. Retallack, J. J. Veevers, R. Morante, *Geol. Soc. Am. Bull.* **108**, 195 (1996).
15. A. Hallam, *Hist. Biol.* **5**, 257 (1991).
16. P. B. Wignall, R. J. Twitchett, in *Catastrophic Events and Mass Extinctions: Impacts and Beyond*, C. Koeberl, K. G. MacLeod, Eds. (Geological Society of America, Boulder, CO, 2002), pp. 395–413.
17. M. Magaritz, R. Bar, A. Baud, W. T. Holser, *Nature* **331**, 337 (1988).
18. A. Baud, M. Magaritz, W. T. Holser, *Geol. Rundsch.* **78**, 649 (1989).
19. E. S. Krull, G. J. Retallack, *Geol. Soc. Am. Bull.* **112**, 1459 (2000).
20. K. Wang, H. H. J. Geldsetzer, H. R. Krouse, *Geology* **22**, 580 (1994).
21. M. J. de Wit *et al.*, *J. Geol.* **110**, 227 (2002).
22. W. S. Broecker, S. Peacock, *Global Biogeochem. Cycles* **13**, 1167 (1999).
23. N.-V. Atudorei, thesis, University of Lausanne (1999).
24. A. Baud, V. Atudorei, Z. D. Sharp, *Geodin. Acta* **9**, 57 (1996).
25. V. Atudorei, A. Baud, *Albertiana* **20**, 45 (1997).
26. D. J. Lehrmann, J. Wei, P. Enos, *J. Sediment. Res.* **68**, 311 (1998).
27. M. W. Martin *et al.*, *GSA Abstr. Program* **33**, 201 (2001).
28. Materials and methods are available as supporting material on *Science* Online.
29. M. Horacek, R. Brandner, R. Abart, paper presented at the 3rd Viennese Workshop on Stable Isotopes in Biological and Environmental Sciences, Vienna, Austria, 9 November 2001.
30. J. Tong, Y. D. Zakharov, M. J. Orchard, H. F. Yin, H. J. Hansen, *Sci. China Ser. D Earth Sci.* **46**, 1182 (2003).
31. Y. G. Jin *et al.*, *Science* **289**, 432 (2000).
32. A. R. Basu, M. I. Petaev, R. J. Poreda, S. B. Jacobsen, L. Becker, *Science* **302**, 1388 (2003).
33. L. Becker *et al.*, *Science* **304**, 1469; published online 13 May 2004 (10.1126/science.1093925).
34. S. L. Kamo *et al.*, *Earth Planet. Sci. Lett.* **214**, 75 (2003).
35. R. A. Berner, *Proc. Natl. Acad. Sci. U.S.A.* **99**, 4172 (2002).
36. G. R. Dickens, J. R. O'Neil, D. K. Rea, R. M. Owen, *Paleoceanography* **10**, 965 (1995).
37. D. P. Schrag, R. A. Berner, P. F. Hoffman, G. P. Halverson, *Geochem. Geophys. Geosyst.* **3**, 10.1029/2001GC000219 (2002).
38. At an organic carbon burial rate of 20 Gt of C per ky (similar to the present-day rate), if 1% of all organic carbon buried were converted to methane and stored as gas hydrate (a high estimate), then only 200 Gt of C would accumulate as methane hydrate per million years.
39. A. J. Kaufman *et al.*, *Geol. Mag.* **133**, 509 (1996).
40. M. D. Brasier, G. Shields, V. N. Kuleshov, E. A. Zhegallo, *Geol. Mag.* **133**, 445 (1996).
41. E. Ott, *Neues Jahrb. Geol. Palaeontol. Abh.* **141**, 81 (1972).
42. B. Senowbari-Daryan, R. Zuhlke, T. Bechstadt, E. Flügel, *Facies* **28**, 181 (1993).
43. S. L. Romano, S. D. Cairns, *Bull. Mar. Sci.* **67**, 1043 (2000).
44. R. Mundil, P. Brack, M. Meier, H. Rieber, F. Oberli, *Earth Planet. Sci. Lett.* **141**, 137 (1996).
45. E. Flügel, in *Phanerozoic Reef Patterns*, W. Kiessling, E. Flügel, J. Golonka, Eds. (Society for Sedimentary Geology, Tulsa, OK, 2002), pp. 391–464.
46. J. J. Sepkoski, *Bull. Am. Paleontol.* **363**, 1 (2002).
47. We thank Y.-Y. Yu, J. Xiao, H. Yao, A. Bush, and R. Kodner for assistance in the field; G. Escheid for laboratory assistance; and R. Bambach, G. Dickens, P. Koch, P. Enos, D. Erwin, and three anonymous reviewers for constructive comments on the manuscript. Supported by NSF [grant nos. EAR-9804835 to D.J.L. and OCE-0084032 to A.H.K., project EREUPT (Evolution and Radiation of Eukaryotic Phytoplankton)], the American Chemical Society (grant no. ACS-PRF 33122-B8 to D.J.L.), a Sigma Xi Grant-in-Aid of Research to J.L.P., a National Defense Science and Engineering Graduate Fellowship to J.L.P., and the Geological Survey of Canada (Project CCGK4700, contribution no. 2003314 to M.J.O.).

Ecosystem Properties and Forest Decline in Contrasting Long-Term Chronosequences

David A. Wardle,[1,2]* Lawrence R. Walker,[3] Richard D. Bardgett[4]

During succession, ecosystem development occurs; but in the long-term absence of catastrophic disturbance, a decline phase eventually follows. We studied six long-term chronosequences, in Australia, Sweden, Alaska, Hawaii, and New Zealand; for each, the decline phase was associated with a reduction in tree basal area and an increase in the substrate nitrogen–to-phosphorus ratio, indicating increasing phosphorus limitation over time. These changes were often associated with reductions in litter decomposition rates, phosphorus release from litter, and biomass and activity of decomposer microbes. Our findings suggest that the maximal biomass phase reached during succession cannot be maintained in the long-term absence of major disturbance, and that similar patterns of decline occur in forested ecosystems spanning the tropical, temperate, and boreal zones.

After catastrophic ecosystem disturbance, primary succession occurs; this involves an initial period of ecosystem development leading to a maximal biomass stage. The build-up phase has been extensively studied and is characterized by broadly predictable changes in ecosystem productivity, biomass, nutrient availability, and soil processes (*1–4*). However, in the prolonged absence of catastrophic disturbance in either late primary or secondary succession, a decline or regressive phase often follows, during which there is a significant reduction in ecosystem productivity and standing plant biomass (*5–7*). Unlike the build-up phase, the decline phase and associated ecosystem-level changes are poorly understood. Yet an improved understanding of this decline phase is essential for evaluating the mechanistic basis of forest decline as well as the long-term importance of disturbance in maintaining ecosystem properties and processes.

Here we assess changes that occur in several properties that can be related to the functioning of ecosystems in the long term (that is, on the order of at least several thousand years) along each of six well-established chronosequences (Table 1, table S1, and fig. S1). Each chronosequence represents a series of sites varying in age since surface formation or catastrophic disturbance, but with all other extrinsic driving factors being relatively constant. In any chronosequence, the older stages would previously have been subjected to climatic regimes that were different from the present regime; however, our study seeks only to relate ecosystem properties under the present climatic regime to substrates of varying ages since their formation. Each of the six sequences has previously been shown to endure long enough for a decline in standing plant biomass to occur. They range from 6000 to over four million years old and represent a range of locations, macroclimatic conditions, parent materials, and agents of disturbance forming the chronosequence.

[1]Department of Forest Vegetation Ecology, Swedish University of Agricultural Sciences, SE901 83 Umeå, Sweden. [2]Landcare Research, Post Office Box 69, Lincoln, New Zealand. [3]Department of Biological Sciences, Box 454004, University of Nevada, Las Vegas, 4505 Maryland Parkway, Las Vegas, NV 89154–4004, USA. [4]Institute of Environmental and Natural Sciences, Lancaster University, Lancaster LA1 4YQ, UK.

*To whom correspondence should be addressed. E-mail: david.wardle@svek.slu.se